PHILOSOPHICAL TRANSACTIONS OF THE ROYAL SOCIETY A
MATHEMATICAL, PHYSICAL & ENGINEERING SCIENCES

Integrated Circuit Metrology with Confocal Optical Microscopy [and Discussion]

S. D. Bennett, J. T. Lindow, I. R. Smith, R. B. Thompson and H. N. G. Wadley

Phil. Trans. R. Soc. Lond. A 1986 **320**, 307-313
doi: 10.1098/rsta.1986.0119

Phil. Trans. R. Soc. Lond. A **320**, 307–313 (1986)
Printed in Great Britain

Integrated circuit metrology with confocal optical microscopy

By S. D. Bennett, J. T. Lindow and I. R. Smith
Si-Scan Systems, 911 *Dell Avenue*, *Campbell*, *California* 95008, *U.S.A.*

An experimental investigation of contrast in confocal optical micrographs of semiconductor wafers is presented. Results show a smooth variation of contrast over the edges of deposited layers as the focal plane is varied: correct interpretation of this contrast may enhance the accuracy of edge detection and hence of line-width measurement.

INTRODUCTION

The semiconductor industry relies on high-resolution microscopy for the inspection and measurement of devices. Although scanning electron microscopes are capable of high-resolution imaging they are not the instrument of choice for production control; the vacuum requirements limit throughput, and the use of low accelerating voltage (to reduce the effects of charging dielectric surfaces) results in poor signal:noise ratios. Traditional methods with optical microscopes have been found inadequate for line widths below approximately 1.5 μm, particularly as the width, registration and distortion tolerances required for 'state of the art' devices are shrinking even faster than the line widths themselves.

The confocal scanning microscope (CSM; Brakenhoff 1981; Sheppard 1981) provides a natural extension to the performance of optical inspection techniques. Increased resolution both from the confocal properties of the system and from the use of short-wavelength coherent light make it an appropriate basis for an automated inspection system that we have developed.

As with all imaging systems, a key factor in judging their usefulness lies in determining the relation between image and object, an understanding of this relation is essential if accurate line-width measurements are to be made from the image. In particular, we are concerned with the precision detection and location of lateral boundaries on the object. Once these are located we can make measurements based on an accurate knowledge of the spatial magnification of our system. In this paper we will discuss how present theoretical treatments of the imaging performance of the CSM relate to the semiconductor metrology problem, and highlight areas where they are apparently inadequate. We will also discuss experimental results that suggest that departures from theoretical behaviour are surprisingly small and lead us to suppose that a revised approximate model need not be unduly complex.

OPTICAL CONTRAST AT BOUNDARIES

The measurement of line width cannot be divorced from the behaviour of the imaging system in the vicinity of diffracting boundaries. It is not easy to analyse this situation in any detail when the specimen is three dimensional and the probe beam is highly focused. We will discuss here three instances: first, the idealized situation where there is no topography, second, the situation of such large topography that the top of the feature is essentially isolated in space, and finally, the situation of practical interest, where the topography of the feature is comparable with the depth of field of the imaging system.

Planar specimen

The situation illustrated in figure 1*a* has been studied in considerable detail by several authors both in the context of scanning optical and acoustic microscopy (Bullis & Nyyssonen 1982; Atalar 1978; Wickramasinghe 1978; Lemons 1975; Sheppard & Wilson 1978*a*). The specimen has no topography and therefore gives a step response which may be predicted theoretically. Specimens that approximate closely the conditions illustrated are available: for example, a chrome on glass photolithography mask has reflectivities of over 95% and less than 4% respectively, with layer thickness of a few tens of nanometres. A typical edge-response curve for our experimental system is shown in figure 2, in good agreement with theory. The wavelength used in these experiments was 442 nm and the numerical aperture of the objective lens was 0.9.

The specimen used for this experiment had a number of accurately etched lines and spaces on it. We measured the width of the structure, using 25% of the peak intensity excursion as the criterion for locating the physical edge of the sample, as predicted by theory (Sheppard & Choudhoury 1978). We consistently achieve excellent agreement between measurement and known line width with this type of sample. Accuracy of 5 nm and repeatability of 1 nm are typical for lines down to 0.5 μm wide. This further illustrates the ideal nature of this particular sample configuration. While this situation is realized for a photolithography mask, it is very far removed from the practical example of a semiconductor wafer with real device structure.

Specimen with large topography

Figure 1*b* illustrates the situation where topography exists. We assume now that the topography is much greater than the depth of field of the microscope. This too is something of an idealization but it is useful for our discussion. It is readily appreciated that when the focal plane is arranged to be coincident with the top surface of the specimen, the edge response is rather simple, and indeed may be theoretically predicted: it is very like the planar specimen. The CSM has smaller depth of field than the conventional microscope (Sheppard & Wilson 1978) and this is exploited in semiconductor measurements. The axial response of our system, the so called $V(z)$ curve, has been optimized to give the narrowest possible mainlobe. The theoretical mainlobe width at the half-power points for our instrument is 0.41 μm; we find a width of 0.45 μm experimentally.

By making use of this very narrow depth of field we may focus the instrument on the layer to be measured and so the conditions more closely correspond to the planar specimen. In this situation it is possible to make line-width measurements for the top part of the structure and to make pitch measurements in a similar manner. If the side walls of the line were vertical this would be sufficient information also to determine the width of the space. Unfortunately, in practice the side walls vary in slope from *ca.* 90° to as little as 70°. In devices built with 1.0 μm design rules, a slope of 70° would be sufficient to broaden the base of the line by more than the 10% typical line-width tolerance. Once again, this would be acceptable if the slope were accurately known and invariant. However, in practice the slopes do vary owing to process drifts, and it is vital to be able to measure the width at the bottom of the structure as well as at the top; the bottom, after all, generally represents the electrically significant dimension. It is clearly possible to focus on the top structure in a region well away from the edge and then again on the substrate also well away from the edge. The very sharply defined axial response of the

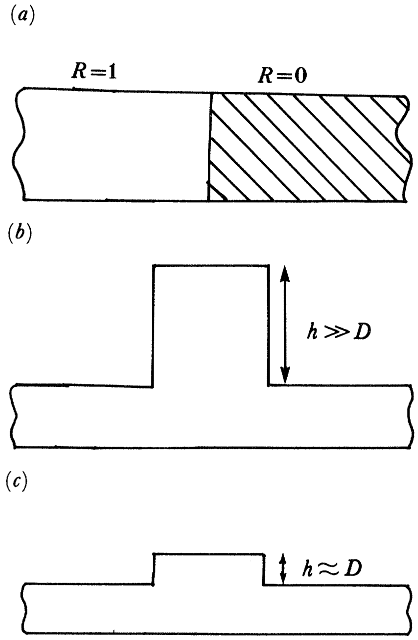

FIGURE 1. The three instances of topography considered. (*a*) Planar sample. (*b*) Topography (height, *h*) much larger than depth of field (*D*). (*c*) Topography of the order of the depth of field.

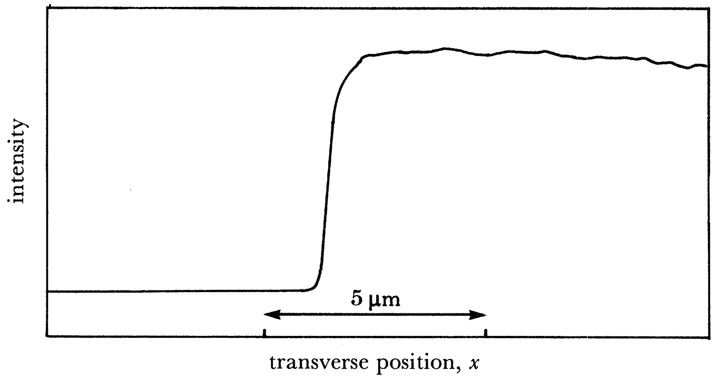

FIGURE 2. Experimental step response for chrome–glass mask, $\lambda = 442$ nm, numerical aperture 0.9.

microscope makes it possible to determine the difference in these two heights to within a few hundred ångströms†. The difficulty lies in discerning the lower edge of the structure.

It should be noted that the behaviour of the $V(z)$ curve in the optical situation is rather different from the acoustic microscope, where material properties dominates the form of the curve (Atalar 1978); in the optical example there is only a small material dependence (Cox *et al.* 1982) and the form of the curve is governed largely by the optical configuration. This can be used to great advantage because the position of the axial peak response in many instances corresponds to the in-focus condition with much less ambiguity than in the acoustic case. Care must, of course, be taken when measuring through transparent films, which distort the beam focus by refraction and also when examining waveguiding films; the latter may be expected to result in $V(z)$ effects similar to those from Rayleigh waves in acoustic microscopy.

---

† 1 Å = 10^{-1} nm = 10^{-10} m.

Topography comparable with the depth of field

The third instance we consider is the practical manifestation of the specimen with large topography. Here the height variation of the layer is comparable with the depth of field of the microscope, figure 1*c*. A few simple observations may illuminate the problem. The form of the edge response is now modified because some signal is returned from the substrate level even when the focal plane is at the top level of the structure. The optical pathlength difference results in a phase cancellation effect, giving a dip in the response around the line edge. The edge response measured for a 0.6 μm silicon dioxide step, shown in figure 3, is a typical example. Furthermore there is a shadowing effect of the edge, figure 4; the lower surface lies in the geometrical shadow region of the edge, which may be simply related to the step height and numerical aperture of the objective lens. In this situation it is not clear what the theoretical relation between the measured edge response and the true edge of the specimen really is.

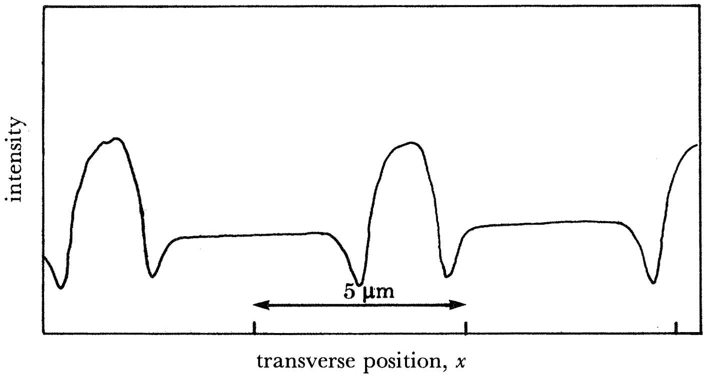

FIGURE 3. Experimental step response for silicon dioxide step (0.6 μm) Silicon substrate; $\lambda = 442$ nm, numerical aperture 0.9.

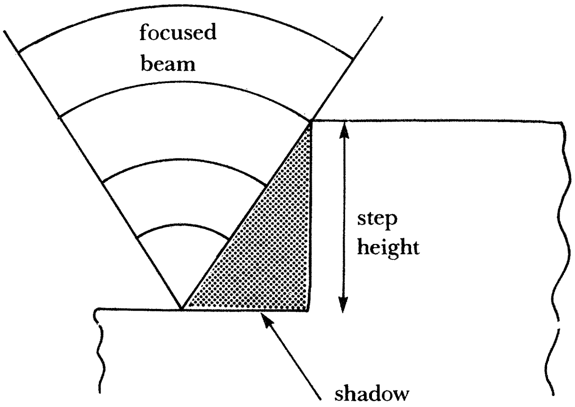

FIGURE 4. Shadow region arising from step. Extent of region depends on numerical aperture and step height.

We have explored this problem experimentally; as yet there is no theoretical model known to the authors that adequately describes this situation. We have examined the behaviour of the $V(z)$ curve in the immediate vicinity of the step for several practical examples, one of which is presented here. It is intuitively clear that the $V(z)$ curve will be well behaved when the optical beam is far removed from the edge on either side. It is much less obvious what behaviour will be observed as z is varied while the beam is positioned directly over the step. Figure 5 shows a series of axial-response curves laterally sampled at approximately $\frac{1}{4}\lambda$ intervals over a silicon dioxide step on a silicon substrate. The SiO_2 layer was 0.6 μm thick, while the axial scan range was 1.8 μm. The somewhat surprising result in figure 5 is that the peak in the response curve moves monotonically and smoothly between the two surface levels. Indeed the profile we would draw by plotting the peak-height location as a function of lateral dimension, figure 6, very closely represents the true surface profile (Hamilton & Wilson 1982*a*, *b*).

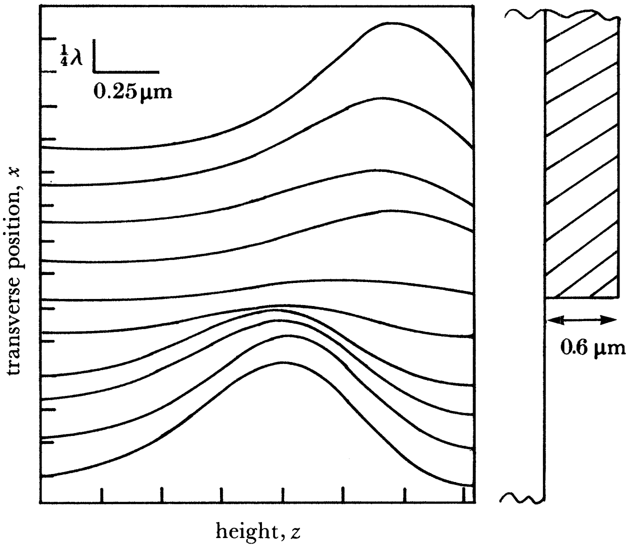

FIGURE 5. $V(z)$ curves plotted in sequence in vicinity of silicon dioxide step, lateral $V(z)$ curve separation $\frac{1}{4}\lambda$. Inset section shows approximate position of step.

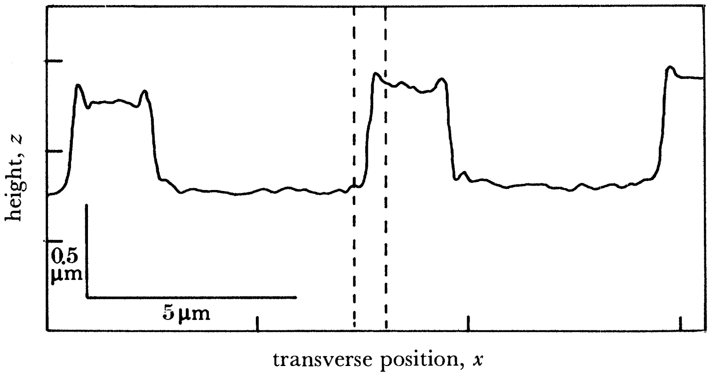

FIGURE 6. Profile resulting from peak location algorithm applied to data used to generate figure 5. Data in figure 5 taken between dotted lines.

DISCUSSION

Intuitively quite complex variations in the $V(z)$ responses measured over a diffracting edge might be anticipated, particularly because the angle of the edge exceeds the half-angle of our objective lens. The simple behaviour that we observe, coupled with the extremely rapid shift in the peak of the $V(z)$ curve, suggests to us that monitoring the form of the $V(z)$ response may be a less ambiguous and possibly more accurate means of locating the lower edge of a layer. This may be reasonable because we are effectively introducing information about the topography of the layer, rather than simply imaging in one plane.

In this study we have made use of only the intensity of the returned signal. Additional information is clearly available if the phase of the reflected signal were recorded. A scheme for exploiting this has been developed by Kino and co-workers (Jungerman *et al.* 1984), although to date their work has concentrated on samples with very little topography.

The simple behaviour observed in our experiment also suggests that it may be accounted for by a relatively simple theoretical model. We note, for example, that if the top surface of the layer is unreflective (or possibly defocused) and the slope of the edge is highly reflective (as it would be for high angles of incidence) then when the beam axis is precisely over the boundary the $V(z)$ response would be simply that of the substrate because the reflecting edge gives symmetry to the situation. We can imagine samples where these conditions might apply, although the situation could hardly be common in practice.

Clearly a full analysis of the edge-detection problem requires a full model. Fortunately in device metrology an absolute error is usually tolerable provided the relative error is small and consistent. In our experimental programme we continue to explore these effects for a range of layer thicknesses, edge slopes and materials. The confocal scanning optical microscope offers better resolution for semiconductor measurement applications and also useful information about the topography of the sample. Combining the topography information with the basic image may further enhance the accuracy of measurement.

The authors are particularly grateful to T. Corl and G. S. Kino of Stanford University for helpful discussions of their related work.

REFERENCES

Atalar, A. 1978 *J. appl. Phys.* **49**, 10.
Brakenhoff, G. T., Binnerts, J. S. & Waldringh, C. L. 1981 In *Scanned image microscopy* (ed. E. A. Ash), pp. 183–200. London: Academic Press.
Bullis, W. M. & Nyyssonen, D. 1982 In *VLSI electronics: microstructure science* vol. 3, (ed. E. D. Einspruch), pp. 301–346. New York: Academic Press.
Cox, I. J., Hamilton, D. K. & Sheppard, C. J. R. 1982 *Appl. Phys. Lett.* **41**, 604–606.
Hamilton, D. K. & Wilson, T. 1982*a* *J. appl. Phys.* **53**, 5321.
Hamilton, D. K. & Wilson, T. 1982*b* *Appl. Phys.* B**27**, 211.
Jungerman, R. L., Hobbs, P. C. D. & Kino, G. S. 1984 *Appl. Phys. Lett.* **45**, 846–848.
Sheppard, C. J. R. & Choudhury, A. 1978 *Optik* **51**, 361–368.
Sheppard, C. J. R. & Wilson, T. 1978*a* *Optica Acta* **25**, 315.
Sheppard, C. J. R. & Wilson, T. 1978*b* *Optics Lett.* **3**, 115–117.
Sheppard, C. J. R. 1981 In *Scanned image microscopy* (ed. E. A. Ash). London: Academic Press.
Wickramasinghe, H. K. 1978 *J. appl. Phys.* **50**, 664.

Discussion

R. B. THOMPSON (*Ames Laboratory, Iowa State University, Ames, Iowa, U.S.A.*). One of the difficulties in interpreting Dr Bennett's images was associated with shadowing of the highly focused beam by steps. Could the situation be improved by a scheme for tilting the sample, and would this be practical?

S. D. Bennett. The shadowing effects certainly are important. The idea of tilting the specimen is a good one; it is used extensively in SEMS. Unfortunately, it is not practical in the optical situation because the short working distance found with high NA lenses and their relatively large physical diameter means that an angle of only a degree or so would be sufficient to cause interference with the sample.

H. N. G. Wadley (*A*163, *Materials Building* 223, *NBS*, *Gaithersburg*, *Maryland*, *U.S.A.*). For periodic structures in particular, spatial Fourier transformation of an image can be used to determine average spacings. Have such approaches been applied to the microelectronic metrology problem Dr Bennett has discussed?

S. D. Bennett. Yes, they have. The confocal microscope lends itself very well to such processing because one is interested in the location of zeros in the spatial frequency domain. The CSM has (ideally) a transfer function with no zeros right out to the cut-off frequency, unlike conventional systems. This has been exploited by Kino and Liang (Kino *et al.* 1985) with the acoustic microscope.

Reference

Liang, K. K., Bennett, S. D., Khuri-Yakub, B. T. & Kino, G. S. 1985 *IEEE Trans. Sonics Ultrasonics* **SU-32** (2), 266–273.